

Determination of the Na/Si(100)2 × 1 surface and interface geometry by polarization-dependent photoemission extended x-ray-absorption fine structure and *ab initio* total-energy molecular calculations

P. S. Mangat

Department of Physics, Northern Illinois University, DeKalb, Illinois 60115-2854

P. Soukiassian* and K. M. Schirm

*Commissariat à l'Energie Atomique, Service de Recherche sur les Surfaces et l'Irradiation de la Matière, Bâtiment 462, Centre d'Etudes de Saclay, 91191 Gif sur Yvette CEDEX, France
and Département de Physique, Université de Paris-Sud, 91405 Orsay CEDEX, France*

L. Spiess,[†] S. P. Tang, and A. J. Freeman

Department of Physics and Astronomy, Northwestern University, Evanston, Illinois 60208-3112

Z. Hurych

Department of Physics, Northern Illinois University, DeKalb, Illinois 60115-2854

B. Delley

Paul Scherrer Institute, c/o RCA Laboratories, Badenerstrasse 569, CH-8048 Zurich, Switzerland

(Received 5 October 1992)

We investigate the structure of the clean and Na-covered Si(100)2 × 1 surface by a combination of the polarization-dependent photoemission extended x-ray-absorption fine-structure (PEXAFS) experimental technique and *ab initio* total-energy molecular method using force calculations (DMOL). We use the unique ability of PEXAFS to measure the distances between the nearest neighbors of both Na adsorbate and Si substrate atoms which allows a double check of interatomic distances. The Na-Si and Si-Si distances are obtained by analyzing the EXAFS signal at the Na 2*p* and Si 2*p* core-level lines. The experimental Na-Si and Si-Si bond lengths are found to be in excellent agreement with the distances obtained by *ab initio* total-energy DMOL calculations performed on very large clusters. The results indicate unambiguously that Na atoms are adsorbed on a single site, the cave. We do not find any Na-Na distance consistent with any of the "double-layer" models. Furthermore, the lowest adsorption energy is found for Na on the cave site. We also probe the fine structural changes of the Si(100)2 × 1 surface upon Na deposition including the Si-Si dimer relaxation. The combination of these experimental investigations and theoretical calculations enables us to get a deeper insight into the understanding of structural properties of alkali-metal/silicon systems and to propose a complete structural model.

I. INTRODUCTION

Structural studies of clean and alkali-metal adsorbate covered Si(100)2 × 1 surfaces and interfaces have been a topic of interest for a few decades due to scientific and technological importance.¹⁻³ New surface-sensitive techniques have aided a better understanding of such systems especially for the structure of clean and alkali-metal-covered surfaces. The atomic geometries of the clean and alkali-metal-covered Si(100)2 × 1 surface were investigated by several experimental techniques such as low-energy electron diffraction (LEED),⁴⁻⁶ photoelectron diffraction using single-scattering analysis (PED),⁷ reflection high-energy electron diffraction (RHEED) measurements,⁸ medium-energy ion scattering (MEIS),⁹ photoemission adsorbed x-ray (PAX),¹⁰ scanning tunneling microscopy (STM),¹¹⁻¹³ surface and/or photoemission absorption fine structure (SEXAFS, PEXAFS),^{14,15} and x-ray standing-wave measurements (XSW).¹⁶ Recent-

ly, several *ab initio* total-energy theoretical calculations using the local density functional approach have also been performed on these systems.¹⁷⁻²⁰ Among them, pseudopotential calculations¹⁸⁻²⁰ have, in general, favored the so-called double-layer model with two adsorption sites for the alkali-metal atoms on the Si(100)2 × 1 surface. This model was first proposed on the footing of PED measurements using a single-scattering analysis, with two adsorption sites, the pedestal and the valley bridge [see Fig. 1(a)].⁷ These results are in opposition to the very recent STM measurements^{11,13} for the prototypical one-monolayer (ML) K/Si(100)2 × 1 surface in which it was shown that K atoms form one-dimensional linear chains distant by 7.68 Å and parallel to the Si dimer rows along the <110> direction with a single adsorption site.¹³ Furthermore, in this later investigation, we have also shown that the presence of impurities, even at very low levels, results in the growth of an additional K layer.¹³ Two decades ago,

Levine, using LEED measurements, proposed the first model of alkali-metal adsorption on a Si(100)2×1 surface for Cs atoms which was found to be adsorbed on a single adsorption site, the pedestal [see Fig. 1(a)], and to form one-dimensional alkali-metal linear chains.⁴ The Levine model was also proposed to be suitable for the K/Si(100)2×1 and Na/Si(100)2×1 systems on the basis of LEED measurements.^{5–7}

The PEXAFS is a variation of the surface EXAFS technique.^{21,22} In this case, the intensity of photoemission from a core level is measured directly as a function of the photon energy. It is now well established that the PEXAFS technique probes the short-range order of atoms in the topmost atomic layer on the surface. The very high surface sensitivity of the method is due to the small escape length ($\approx 5 \text{ \AA}$) of primary photoelectrons in the kinetic energy range of our PEXAFS data. Unlike SEXAFS, PEXAFS allows us to study the local environment of adsorbate as well as substrate atoms. Other advantages of the technique are short data collection time and improved signal-to-noise ratio. Polarization dependent PEXAFS, which enables us to probe bond lengths parallel as well as perpendicular to the surface plane—see Figs. 1(a) and 1(b)—has lately been applied to determine the structure of clean and metal-covered semiconductor surfaces and interfaces.^{23,24}

Recently, we have reported an investigation of the atomic structure of Na/Si(100)2×1 and Cs/Si(100)2×1 systems using *p*-polarized PEXAFS in which we have shown that this technique is applicable to structural investigations of Si(100)2×1 surfaces.¹⁵ The Na-Si distance of $2.80 \pm 0.1 \text{ \AA}$ was obtained from the Na 2*p* PEXAFS data and was found to be the same at low and monolayer Na coverages, close to the sum of Na and Si covalent radii.¹⁵ These results support the model of covalent bonding between Na and Si atoms that we proposed several years ago on the basis of core-level and valence-band photoemission results.^{3,25–27} Our studies also indicated that the alkali metals did not induce significant major changes in the substrate structure. However, since these experiments were performed in *p* polarization [see Figs. 1(a) and 1(b)], the results were primarily more sensitive to bond lengths perpendicular rather than parallel to the surface.

In order to provide deeper insight into the structure of these systems, we have, in this paper, investigated further the structural properties of the clean Si(100)2×1 surface and 1-ML Na/Si(100)2×1 interface by the combination of polarization-dependent PEXAFS experiments and *ab initio* total-energy molecular (DMOL) theoretical calculations. We are able to determine Na-Si and Si-Si distances and, by comparing with DMOL calculations, we show that Na is adsorbed on a single site of adsorption, the cave site, which also has the lowest adsorption energy. We also determine the structural changes of the substrate upon Na adsorption. We did not find any Na-Na bond length perpendicular to the $\langle 110 \rangle$ direction consistent with the existence of a second Na layer. In Secs. II and III we provide the experimental and theoretical details, respectively, while the results are described in Secs. IV and V. Discussion is carried on in Sec. VI.

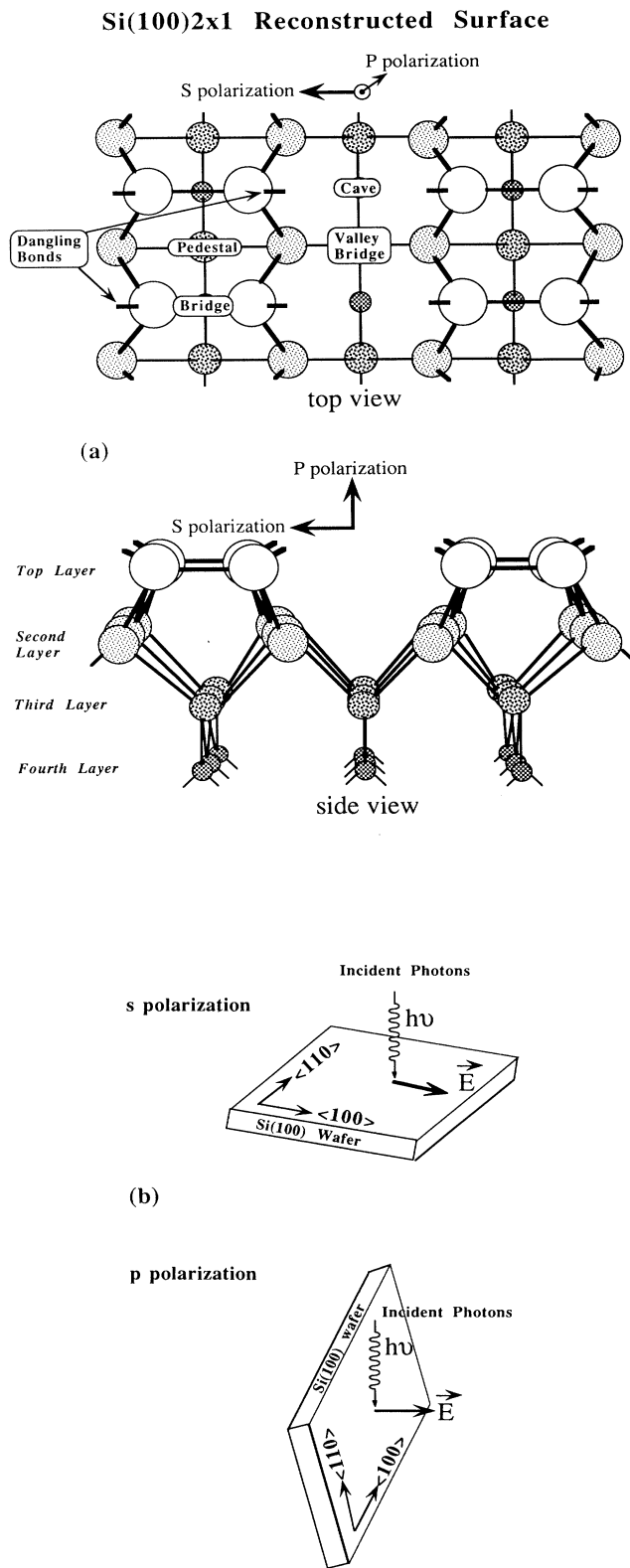


FIG. 1. (a) Schematic top and side views of the reconstructed Si(100)2×1 surface showing the different possible Na adsorption sites. (b) Schematic of the Si(100)2×1 sample set up for *s*- and *p*-polarization PEXAFS.

II. EXPERIMENTAL AND DATA ANALYSIS DETAILS

The PEXAFS experiments were performed at the Synchrotron Radiation Center of the University of Wisconsin–Madison. The radiation emitted by the 1-GeV Aladdin storage ring was dispersed by the “Grasshopper” Mark II monochromator soft x-ray beam line. The ultrahigh-vacuum (UHV) experimental system consisted of an angle integrating double-pass cylindrical mirror analyzer (CMA), crystal cleaver, sample transfer attachment, and a flux monitor system as described elsewhere.¹⁵ During data acquisition, the pressure was better than 5×10^{-11} torr in the ultrahigh-vacuum experimental system and better than 2×10^{-11} torr in the last focusing mirror chamber of the monochromator. The Si(100)2×1 samples were prepared by conventional chemical cleaning process prior to the vacuum treatment. The clean Si(100)2×1 surfaces were obtained by a prolonged thermal annealing of the Si substrate at rather low temperatures followed by rapid thermal annealing cycles at 950°C. During the complete cleaning procedure, the pressure always remained in the low 10^{-10} torr range. The cleanliness of the Si sample was judged from sharp core-level and good valence-band profiles obtained in photoemission with no contamination-related structures. The Na overlayers for interfacial studies were deposited *in situ* at room temperature from a SAES Getter chromate source which was very carefully outgassed prior to alkali-metal deposition in order to avoid any surface contamination. The coverage was monitored by the use of integrated intensity analysis of Na 2*p* and Si 2*p* core levels as described previously.¹⁵ One sodium monolayer (1 ML Na) corresponds to the saturation coverage, i.e., one Na atom per silicon dimer.^{6,15} The pressure increase ∂p during Na evaporation always remained below 2×10^{-11} torr. Using these conditions, no additional Na atoms could be deposited at room temperature beyond the saturation coverage of one sodium monolayer, since the Na sticking coefficient becomes negligible at this point. It is important to notice that the quality of the alkali-metal overlayer, especially the pressure rise during deposition, is of crucial importance for the interpretation of data. We have recently shown that traces of impurities coming from not correctly outgassed SAES alkali-metal sources (pressure increase $\partial p \approx 1.10^{-10}$ torr) during potassium deposition induces the growth of additional K overlayers.^{12,28} We have observed also a similar behavior for the Na/Si(100)2×1 with the clear evidence of growth of a second sodium layer in the presence of impurities at very low level.²⁹ These findings are relevant in view of the present controversies between one-layer and two-layer models and stress the crucial importance of very high standard quality in surface preparation and alkali-metal deposition.^{3,11,13,15,27–29}

For PEXAFS experiments, the photoelectron energies were analyzed by the CMA in the fixed retarding ratio (FRR) mode (pass energy E_p equals kinetic energy E_k) of analyzer operation.^{15,23,24} The photon flux was monitored by collecting the total electron yield from a high transmission grid (transmission >80%) coated *in situ* with lithium fluoride (LiF) with the use of an electrome-

ter and a voltage to frequency (*V-F*) converter. All the acquired data were normalized to the photon flux. The Si 2*p* and Na core-level spectra aid in determining binding energy of the core levels with respect to the valence-band edge, which is required to calculate the constant initial state (CIS) parameters (work function plus binding energy) to obtain the PEXAFS spectra for the absorption edge. The intensity of photoemission from the Si 2*p* core level as a function of the photon energy was monitored in the 115–280-eV photon energy range by a two-point CIS method. The intensity of photoemission from the Na 2*p* core level as a function of the photon energy was monitored in the 80–260 eV photon energy range for 1 ML Na coverage to determine the structure surrounding the Na atom. For the *s*-polarization PEXAFS study, the Si 2*p* and Na 2*p* CIS data were acquired such that the angle between surface normal (SN) and photon electric vector (*E*) of plane polarized incident x rays on the sample was 80°. The advantage of this geometry is that, since the amplitude of EXAFS oscillations is proportional to $\cos^2 a$ [where *a* is the angle between the electric vector of the synchrotron radiation and the vector connecting the atomic pairs of interest—see Figs. 1(a) and 1(b)], the acquired data would be sensitive to the Si-Si dimers. In the two-point CIS method, the data were acquired for one point at the peak and one point in the background (at 5 eV lower binding energy). The experiments were repeated on different surfaces maintaining the same experimental conditions in order to obtain good statistics and check the consistency of the results.

The PEXAFS data were analyzed by the conventional Fourier analysis methods and curve fitting procedures. The two-point CIS data were normalized to the photon flux. The normalized background data were shifted by 5 eV such that the kinetic energy values at each data point for the peak and the background become equal followed by subtraction of the background from the peak. This procedure removes effectively the background as well as any Auger peak, if present, in the spectrum. The data thus obtained represent the absorption coefficient μ .

III. THEORETICAL AND COMPUTATIONAL DETAILS

We have studied the adsorption of Na on the Si(100)2×1 surface with an all-electron numerical method (DMOL) which solves the local density functional equations and derives analytical energy gradients (force calculation). The DMOL method, which uses the finite size cluster model, has been described earlier^{30,31} and already applied to the study of Si(100)2×1 surface.^{17,32} Therefore we will only give here the details of our calculation. We used a double numerical basis set for hydrogen (H) and an extended numerical basis set for Na and Si which includes a double set of valence orbitals and *d*-polarization function. The 1*s*, 2*s*, and 2*p* orbitals were frozen for Si as well as the 1*s* and 2*s* for Na. The 2*p* orbital of Na was not frozen due to recent calculations³³ emphasizing the importance of the partial core correction of the Na atom pseudopotential in the adsorption process. The binding energy of a cluster is defined as

$$E_b = E_t - E_a ,$$

where E_t is the total energy of the cluster and E_a is the sum of each atomic energy. For a given atomic geometry, we have calculated the binding energy of the system and the forces on each atom. To find the optimized geometry, the atoms involved are further displaced according to the forces acting on them. The force convergence criterion is set to 4.0×10^{-3} Ry/a.u. and the degree of convergence for the energy is set to 10^{-5} Ry. In determining the optimum geometry for the different clusters, we restricted ourselves to the geometry which preserves the C_{2v} symmetry.

IV. EXPERIMENTAL RESULTS

A. Si 2p PEXAFS

We first focus on the structures surrounding the Si atoms by looking at the PEXAFS signal at the Si 2p core level. Figure 2 shows the photon energy dependence of Si 2p PEXAFS signal for the clean and 1 ML Na-covered Si(100)2×1 surfaces in *s* polarization—see Figs. 1(a) and 1(b). From the PEXAFS data, the experimental EXAFS modulation function $k^2c(k)$ was obtained. The starting threshold energy (E_0) was taken as 105 eV. The threshold energy E_0 is considered to be a floating parameter and is readjusted later for greater accuracy of results. Figure 3(a) shows the experimental $k^2c(k)$ function for clean and Na-covered Si(100) surfaces. The $k^2c(k)$ data were Fourier transformed to obtain the complex Fourier transform $F(R)$ in the real R space. The absolute $F(R)$ for clean and Na-covered Si(100)2×1 surfaces are shown in Fig. 3(b). The absolute $F(R)$ plot shows peaks near $R = R_j$, where R_j is the interatomic bond length for an atomic pair j (Si-Si, Si-Na, etc.). The peaks represent modified atomic pair distribution function.

For the clean Si(100)2×1 surface, three peaks *A*, *B*, and *C* are observed in Fig. 3(b). Peak *A* represents a single distinct peak as compared to the overlapping peaks *B* and *C*. Peak *A* in $F(R)$ was filtered by a window function $W(R)$ and Fourier backtransformed. The Fourier

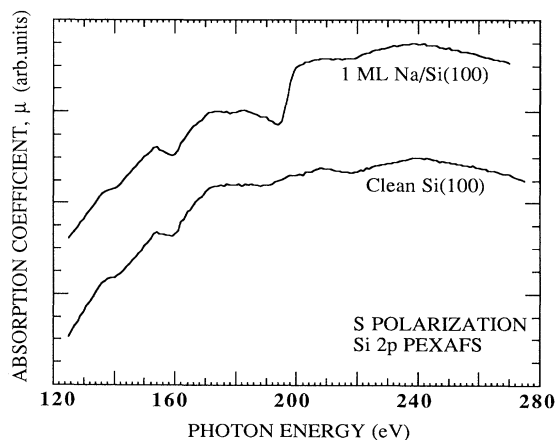


FIG. 2. Si 2p *s*-polarization PEXAFS spectra for clean Si(100)2×1 and 1-ML Na/Si(100)2×1 interface.

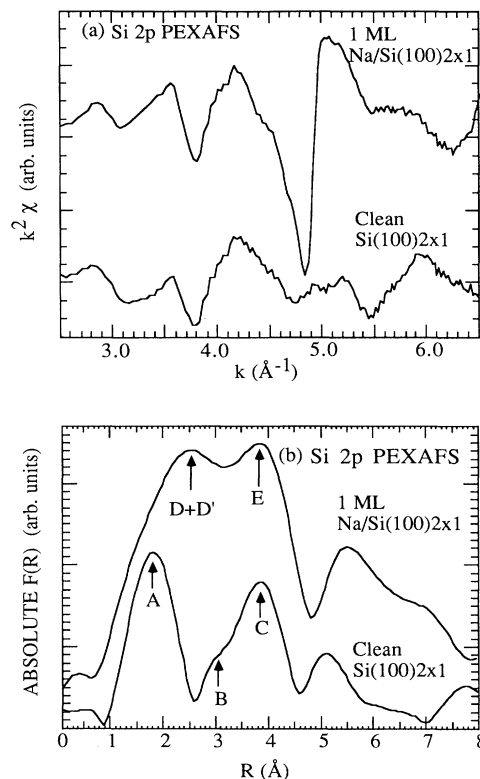


FIG. 3. (a) $k^2\chi(k)$ function for clean Si(100)2×1 and 1-ML Na/Si(100)2×1 interface obtained from Si 2p PEXAFS. (b) Absolute $F(R)$ of the respective EXAFS function for clean Si(100)2×1 and 1-ML Na/Si(100)2×1 interface.

backtransforms yielded a complex function $k^2\chi_A(k)$. The bond length was determined by phase analysis and floating of E_0 according to a procedure reported by Stöhr *et al.*³⁴ The complex $k^2\chi_A(k)$ data were decomposed into phase $[2kR_A + f_A(k)]$ and amplitude $A_A(k)$. The phase function $f_A(k)$ (in this case Si-Si) was calculated using the theoretical absorber (Si) phase function $[f_a(k)]$ of Teo and Lee³⁵ and backscattering (Si) phase function $[f_b(k)]$ of McKale *et al.*³⁶ The calculated phase function for respective absorber-backscatterer atomic pairs was subtracted from the total phase $[2kR_A + f_A(k)]$ to acquire $2kR_A(k)$. At this point, E_0 was floated such that the plot of $2kR_A$ vs k has a zero intercept on the y axis. The slope of $2kR_A$ vs k was divided by two to acquire the interatomic bond length. This procedure resulted in a bond length of 2.20 ± 0.05 Å (see also Table I) which is somewhat shorter than values obtained using classical dynamical LEED measurements (2.40 ± 0.10 Å).⁶ However, our value is in excellent agreement with the *ab initio* DMOL calculation which gives a value of 2.21 Å and will be presented in the next section. The origin of this distance can be explained on the basis of polarization dependence of PEXAFS. Since the data were acquired in the *s*-polarization geometry, the incident photon electric vector is almost parallel and therefore very sensitive to the Si-Si dimer bond length [Fig. 1(a)]. So, this distance is

the Si-Si dimer bond length. Peaks *B* and *C* in Fig. 3(b) for clean Si(100)2×1 surface clearly represent two overlapping peaks. Peaks *B* and *C* in the $F(R)$ were filtered together by a window function $W(R)$, and Fourier backtransformed. The Fourier backtransforms yielded a complex function $k\chi_{B+C}(k)$. Curve fitting procedures were used to determine the Si-Si distances. The experimental $\text{Im}k\chi_{B+C}(k)$ was fit by a model function described by $k[\chi_B(k)] + k[\chi_C(k)]$ where $k[\chi_B(k)]$ is described as $A(k)\sin[2kR_B + f_B(k)]$ and $k[\chi_C(k)]$ can be described as $fA(k)\sin[2kR_C + f_C(k)]$. $A(k)$ is the amplitude function which can be fitted to a single Lorentzian function as described by Teo and Lee and f is described as the fudge factor.³⁵ Theoretical and experimental phase functions were used for the two Si-Si atomic pairs. The complete description of the curve fitting procedures has previously been published in detail elsewhere.^{35,36} Figure 4(a) shows the experimental imaginary $k\chi_{B+C}(k)$ along with the curve fit obtained for the bond length determination. The bond lengths thus computed from the analysis are 3.84 ± 0.1 and 4.60 ± 0.1 Å. They represent the second and third nearest-neighbor distances—see Table I.

When the surface is covered by a Na monolayer (meaning one Na atom per Si dimer), we observe an evident change in the first peak position in absolute $F(R)$ in comparison to the clean surface—Fig. 3(b). The peak appears broader and asymmetric. The peak position is intermediate between peak *A* and peak *B* for the clean surface. Clearly, it has a two-pair distribution function. Thus we label this peak as $D + D'$ for 1 ML Na-covered surface in Fig. 3(b) where *D* and *D'* represent Si-Si and

Si-Na atomic pair distribution. The determination of Si-Si and Si-Na bond lengths required curve fitting procedures. The bond lengths thus determined are 2.44 ± 0.05 Å for the Si-Si atomic pair and 2.67 ± 0.05 Å for the Si-Na atomic pair. Figure 4(b) shows the experimental $k\chi_{D+D'}(k)$ along with curve fit. Peak $D + D'$ was also fit assuming *D'* to be the Si-Si atomic pair but better fit was obtained for the Si-Na atomic pair, which suggests that *D'* is related to a Si-Na atomic pair. The observed values of the bond distances are of particular interest. The Si-Si distance of 2.44 ± 0.05 Å indicates that there is relaxation by 0.24 Å in the Si-Si dimers due to the sodium deposition. The Si-Na distance of 2.67 ± 0.05 Å corresponds to the sum of covalent radii of Si atom (1.11 Å) and Na atom (1.57 Å) thereby supporting the model of covalent bonding between Na and Si established before from the electronic properties on the footing of our photoemission experiments.^{25–27} One should also notice that this bond length is in very good agreement with the one measured at 2.80 ± 0.10 Å using *p*-polarized Na 2*p* PEXAFS.¹⁵ It is important to remark that it was not possible to obtain the Si-Na bond length from *p*-polarized Si 2*p* PEXAFS. Moreover, in the *p*-polarization study, the Na-Si bond distance was obtained from the Na 2*p* PEXAFS which gives structure surrounding the Na atom.¹⁵ At this point, it is interesting also to mention that the Si-Na distance measured here by *s*-polarization PEXAFS indicates that the Si-Na bond direction makes a very small angle with the incident photon electric vector thereby contributing more to the EXAFS oscillations. This suggests that the Si-Na bond is more “horizontal” than “vertical” which does not favor a pedestal (or

TABLE I. Experimental and theoretical bond lengths. For PEXAFS experiment: (a) $R_1(\text{Si})$ and $R_2(\text{Si})$ indicate the first and second nearest-neighbor distances surrounding the Si atom obtained from Si 2*p* PEXAFS. (b) $R_1(\text{Na})$ and $R_2(\text{Na})$ indicate the first and second nearest-neighbor distances surrounding the Na atom obtained from the Na 2*p* PEXAFS. For DMOL calculations: (c) d_1 and d_4 indicate the first and fourth nearest distances between Na and Si atoms. The number between brackets after the bond lengths (1) indicates the number of the atomic layer from the top of Si(100)2×1 surface.

(a)					
Si 2 <i>p</i> PEXAFS	Si dimer $R_1(\text{Si})$	$R_2(\text{Si})$	$R_3(\text{Si})$	$R_4(\text{Si})$	
Clean Si(100)2×1	(<i>A</i>) 2.20 ± 0.04 Å (Si-Si)		(<i>B</i>) 3.84 ± 0.06 Å (Si-Si)	(C) 4.60 ± 0.08 Å (Si-Si)	
Na/Si(100)2×1 (1 Na monolayer)	(<i>D</i>) 2.44 ± 0.04 Å (Si-Si)	(<i>D'</i>) 2.67 ± 0.05 Å (Si-Na)	(<i>E</i>) 3.90 ± 0.08 Å (Si-Si)		
(b)					
Na2 <i>p</i> PEXAFS	$R_1(\text{Na})$		$R_2(\text{Na})$		
Na/Si(100)2×1 (1 Na monolayer)	(A) 2.67 ± 0.05 Å ^a (Na-Si)		(B') 5.10 ± 0.10 Å (Na-Si)		
(c)					
DMol	(Si-Si)	d_1 (Na-Si)	d_2 (Na-Si)	d_3 (Na-Si)	d_4 (Na-Si)
Clean Si(100)2×1	2.21 Å				
Na/cave	2.34 Å	2.86 Å (1)	3.59 Å (2)	3.94 Å (3)	5.11 Å (1)
Na/pedestal	2.26 Å	3.03 Å (1)	3.62 Å (2)	4.51 Å (3)	5.26 Å (2)
Na/valley bridge	2.31 Å	3.02 Å (2)	3.48 Å (1,3)	4.86 Å (2)	5.19 Å (3)

^a 2.80 ± 0.10 Å measured in *p* polarization (Ref. 15).

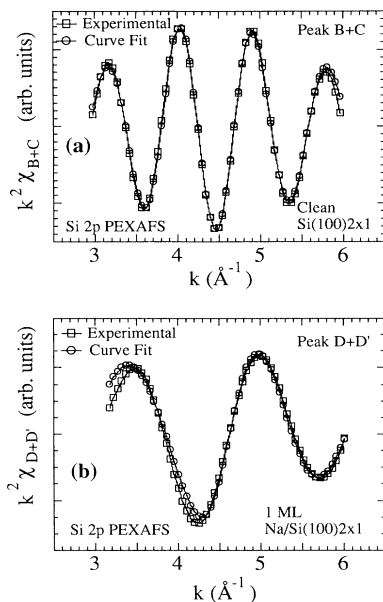


FIG. 4. (a) Imaginary part of the experimental complex $k^2 \chi_{B+C}(k)$ (square) and curve fit (circle) for peak $B+C$ shown in Fig. 3(b) for clean Si(100)2 \times 1 surface. (b) Imaginary part of the experimental complex $k^2 \chi_{D+D'}(k)$ (square) and curve fit (circle) for peak $D+D'$ shown in Fig. 3(b) for 1-ML Na/Si(100)2 \times 1 interface.

bridge) site of adsorption for the Na atom.⁴ The peak E observed in the $F(R)$ for 1-ML Na/Si(100)2 \times 1 yields [Fig. 3(b)] a bond distance of 3.90 ± 0.06 \AA using Si-atom (absorber) and Si-atom (backscattered) phase function, which is related to the second nearest-neighbor Si-Si distance.

B. Na 2p PEXAFS

We now examine the structure surrounding the Na atom from Na 2p PEXAFS for 1-ML Na/Si(100)2 \times 1 interface. Figure 5(a) shows the Na 2p EXAFS function and Fig. 5(b) the respective absolute Fourier transform of the EXAFS function. The starting threshold energy for the EXAFS function was 30 eV and was floated later in the analysis as explained earlier. From the peaks observed in the absolute Fourier transform in Fig. 5(b), we notice two major distinct peaks and we label these as peaks A and B . We analyzed these peaks in the absolute Fourier transform using the Na(absorber)–Si(backscatterer) phase function obtained from the theoretical absorber phase function of Teo and Lee³⁵ and backscattering phase function of McKale *et al.*³⁶ The Na-Si distance obtained for peak A is 2.67 ± 0.05 \AA [see Table I(b)]. From peak B , the distance obtained using Na-Si phase function is 5.10 ± 0.1 \AA , which is the second Si atom distance from the Na atom—see also Table I(b). Furthermore, one should also mention that we do not find any Na-Na distance around 4 \AA , which could be consistent with any of the double-layer models^{7–10, 18–20} (4.4

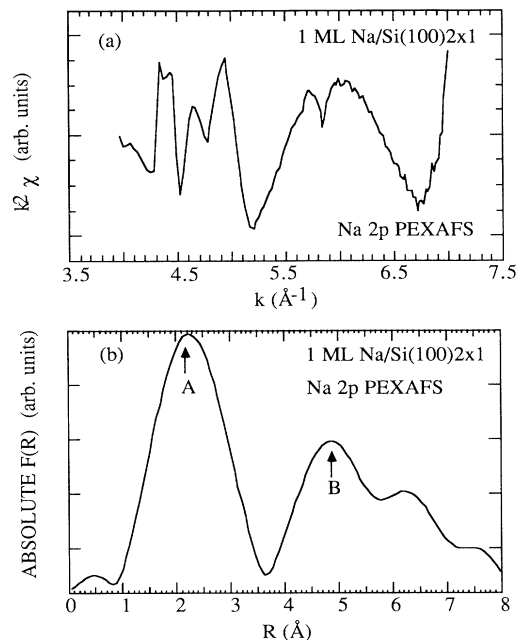


FIG. 5. (a) $k^2 \chi(k)$ function for 1-ML Na/Si(100)2 \times 1 interface obtained from Na 2p PEXAFS. (b) Absolute $F(R)$ of the respective EXAFS function for 1-ML Na/Si(100)2 \times 1 interface.

\AA between pedestal and cave sites and 3.9 \AA between pedestal and valley-bridge sites). It is also interesting to notice that we find the Na-Si bond length (measured using Na 2p PEXAFS) to be strictly equal to the Si-Na bond length (measured using Si 2p PEXAFS) at 2.67 ± 0.05 \AA . It shows a unique feature of the PEXAFS technique in its ability to *double-check* interatomic distances.

V. THEORETICAL CALCULATIONS

A. Study of the clean Si(100)2 \times 1 reconstructed surface

We now turn to the results given by the theoretical DMOL calculations. Since it is possible that surface relaxation might be of some relevance in the determination of the correct adsorption site, we also have to take into account this parameter to figure out its relative importance. Therefore, in order to have a clear understanding of the relaxation, we have first studied the structure of the reconstructed clean surface on different sites. The purpose of obtaining the reconstructed geometry of the clean surface is to have minimization of the forces acting on the atoms of the substrate to the criterion of convergence, so that the forces created on the Si atoms by Na adsorption will have no contribution from nonoptimized substrate forces. For the investigation of the reconstruction, three models were chosen to simulate the dimer and substrate, with hydrogen atoms used as a classical procedure to saturate the dangling bonds. The three clusters are centered on the pedestal, cave, and valley-bridge sites

with 71, 59, and 71 atoms, respectively, including five to six layers of Si—see Figs. 6(a), 6(b), and 6(c). The sizes of the clusters are chosen so that the center atoms are in a good crystal environment (which is not the case for the cluster boundary atoms). Thus choosing three clusters centered on different parts of the unit cell allows us to give a good description of the forces and geometry optimization on all atoms of the unit cell.

The degrees of freedom for the geometry optimization are the following: for all layers, the y axis is frozen as a result of the 2×1 symmetry reconstruction and previous analysis.^{32,37} The first and second layers are allowed to relax along the x and z axes and the third layer along the z axis. The atoms below are kept in their bulk position. Although it has been shown³⁷ that the reconstruction may affect the substrate up to the fourth layer, we have chosen to freeze it, in order to avoid boundary effects from the bottom of the clusters. We have found a reconstructed geometry consistent with the three clusters represented in Figs. 6(a)–6(c). The dimer bond length for the clean Si(100)2×1 surface was found to be 2.21 Å on all three clusters, in excellent agreement with the experimental value given above at 2.20 ± 0.05 Å by PEXAFS—see Table I. Our calculated value agrees well with the one given recently by Tang, Freeman, and Delley³² at 2.23 Å with a cluster centered on the bridge site that we therefore did not study again in this paper.

B. Na adsorption on the Si(100)2×1 surface

In order to have a better representation of dimers and substrate relaxation for each site (i.e., minimization of the

boundary effects), we have built three new clusters embedding in each case two identical adsorption sites lined up perpendicularly to the dimer rows. Each site was studied with the adsorption of two Na atoms per cluster, with 71, 65, and 77 atoms for the pedestal, cave, and valley-bridge sites, respectively—see Figs. 7(a), 7(b), and 7(c). It should be noticed that the two sodium atoms on each cluster are separated by 7.68 Å and are located on different rows. Therefore we expect a negligible contribution of the Na-Na interaction to the binding energy. This was further confirmed in our calculation. Moreover, having two Na atoms per cluster enables us to claim for the representation of a higher coverage model of the surface and thus to be able to compare our calculations with the experimental values. We have plotted in Table I(c) the relaxed bond lengths of the Na atom with the four nearest-neighbor Si atoms for each site of adsorption, together with the relaxed Si-Si dimer bond length (the numbers in brackets refer to the layer of the Si atom).

The geometry optimization, based on force calculation, has shown that the Na-induced substrate relaxation mainly affects the dimers. On the cave site, where the relaxation is most important, the dimers relax upwards by 0.16 Å and are stretched apart by 0.13 Å, while second- and third-layer atoms relax less than 0.02 Å. Thus a simple comparison of the relaxed dimer bond length with that of the clean surface gives a correct knowledge of the importance of the relaxation on each site. Relaxation on the valley-bridge site is similar to that of the cave site, with the same directions of displacement for the Si dimer atoms and no significant effect under the first layer. It can be seen that, unlike the cave and valley-bridge sites,

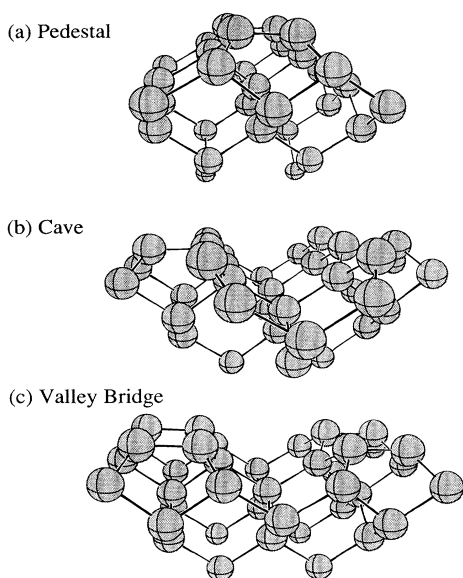


FIG. 6. Clusters used in the calculation to study the clean Si(100)2×1 surface. Each cluster is centered on one of the Na possible adsorption sites: (a) Pedestal, $\text{Si}_{31}\text{H}_{28}$, (b) cave, $\text{Si}_{35}\text{H}_{36}$, and (c) valley bridge, $\text{Si}_{39}\text{H}_{32}$. The hydrogen atoms are not represented.

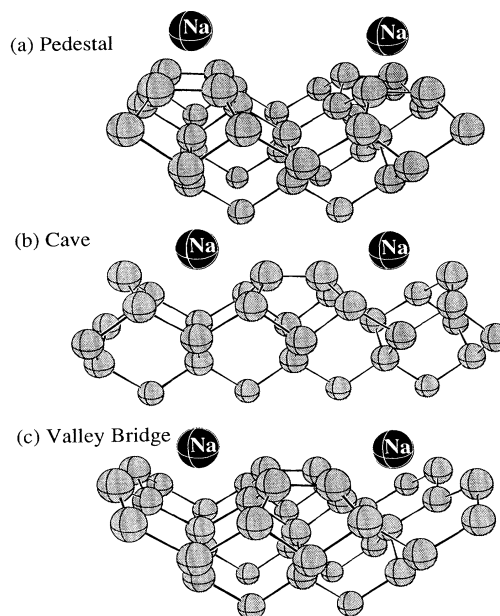


FIG. 7. Clusters used in the calculation to study the various Na adsorption sites: (a) Pedestal, $\text{Si}_{39}\text{H}_{32}\text{Na}_2$, (b) cave, $\text{Si}_{31}\text{H}_{34}\text{Na}_2$, and (c) valley bridge, $\text{Si}_{39}\text{H}_{38}\text{Na}_2$. The hydrogen atoms are not represented.

the pedestal site does not undergo a strong relaxation: dimers move 0.03 Å upwards and are 0.05 Å stretched apart.

It should be noticed first that, for the Na atom on the valley-bridge site, the first nearest neighbor is the second-layer Si atom. This characteristic of the valley-bridge site implies some significant ionicity of the Na-Si bonding, since the second-layer Si atoms are saturated. This does not agree with recent experiment emphasizing a covalent Na-Si bond.^{15,25–27} For the first neighbor distances the cave site has the best fit (2.86 Å) to the experimental distance of 2.67 ± 0.05 Å and differs from the two other values by 0.17 Å.³⁸ Also, the fourth nearest Na-Si distance (d_4) for the cave site is in excellent agreement with the experimental Na 2*p* PEXAFS value of $R_2(\text{Na})$ at 5.10 ± 0.10 Å, unlike the corresponding distances for the pedestal (5.26 Å) and valley-bridge (5.19 Å) sites (see Table I).

The Na adsorption energies per atom are shown in Table II for each absorption site. For the case of unrelaxed substrate, the cave site has the lowest adsorption energy followed closely by the pedestal site with a difference of 0.04 eV. The energy difference is too small to build a reliable conclusion on the correct site of adsorption on the basis of unrelaxed calculation only. The valley-bridge site has an adsorption energy 0.31 eV higher. We now consider substrate relaxation obtained using force calculations. The cave site undergoes a significant relaxation which lowers the energy by 0.19 eV compared to 0.06 and 0.20 for the pedestal and valley-bridge sites, respectively. Thus the cave site has now the lowest adsorption energy after relaxation (0.17 eV lower than the pedestal, which is a significant difference). Although the valley-bridge site has a comparable lowering of the adsorption energy due to the relaxation, it remains 0.30 eV higher than the cave site.

The calculation was repeated with three Na atoms adsorbed on cave sites on a line perpendicular to the dimer rows along the $\langle 110 \rangle$ direction, in order to trace the effect of increasing the number of Na atoms and to check consistency of our results. The cluster contains 37 Si, 38 H, and 3 Na atoms and is represented in Fig. 8. The results are in excellent agreement with the calculations performed using two Na-atom clusters (Fig. 7). In this case, the relaxed adsorption energy is 2.23 eV compared to 2.22 eV for two Na atoms and all the relaxed bond lengths were within 0.03 Å of the values obtained previously.

TABLE II. Na-adsorption energies for the cave, pedestal, and valley-bridge sites in the cases of unrelaxed and relaxed Si(100)2×1 substrate.

DMOL	Na adsorption	
	Unrelaxed	Relaxed
Cave	−2.03 eV	−2.22 eV
Pedestal	−1.99 eV	−2.05 eV
Valley bridge	−1.72 eV	−1.92 eV

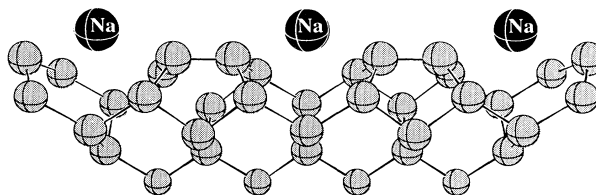


FIG. 8. Cluster used in the calculation to simulate three Na atoms adsorbed on cave sites: $\text{Si}_{37}\text{H}_{38}\text{Na}_3$. The hydrogen atoms are not represented.

VI. DISCUSSION

The present results show that the Si-Si dimer bond is 2.20 ± 0.05 Å on the clean Si(100)2×1 surface, which is somewhat shorter than the value obtained recently by dynamical LEED measurements at 2.4 ± 0.1 Å.⁶ However, the experimental measurement using *s*-polarization Si 2*p* PEXAFS is in excellent agreement with the above *ab initio* total-energy DMOL calculation giving practically the same value at 2.21 Å. Upon the deposition of a sodium monolayer, the PEXAFS results indicate that the Si-Si dimer is relaxed by 0.24 Å at 2.44 Å. The agreement with the calculations is found to be better for the cave site at 2.34 Å,³⁹ than for the pedestal site at 2.26 Å and the valley-bridge site at 2.31 Å, and close to the value obtained by dynamical LEED measurements.⁶ This relaxation is likely to result from electron redistribution at the Na-Si interface as a consequence of the hybridization between the Na 3*s* valence electron with the Si 3*p* orbital related to the dangling bond leading to the formation of a covalent bonding as shown previously on the basis of photoemission experiments.^{3,26} The Si-Si dimer relaxation by 0.24 Å also indicates a weakening of the dimer bonding which is consistent with a different equilibrium in the electronic structure as described above. Our results do not indicate any other major structural changes within the (100) surface of silicon upon Na deposition which is in very good agreement with the previous *p*-polarized PEXAFS measurements.¹⁵ This is significantly different from the behavior of the InP(110) surface on which Na was found to induce significant structural changes, even at rather low coverages.²² This limited change of the Si(100)2×1 surface is likely to result from the fact that the covalent bonding between Na and Si is weak.^{3,15,26}

In our previous *p*-polarized PEXAFS experiments¹⁵ we were not able to use the Si 2*p* (unlike the Na 2*p*) to measure the Na-Si bond length. It is interesting to notice here that we have also used and analyzed the EXAFS oscillations in *s* polarization at both Na 2*p* and Si 2*p* to measure the Na-Si as well as the Si-Na bond lengths. The results are identical in both cases at 2.67 ± 0.05 Å, which corresponds to the sum of Na (1.57 Å) and Si (1.11 Å) covalent radii as measured for the 1-ML K/Si(100)2×1 interface by SEXAFS.¹⁴ This value is in very good agreement with the result given by *p*-polarized PEXAFS at 2.80 ± 0.10 Å (Ref. 15) and with the bond length calculat-

ed by DMOL for the cave site at 2.86 Å (d_1 in Fig. 9). Again, the agreement is less good with the bond length calculated for the pedestal (3.03 Å) and valley-bridge (3.02 Å) sites. If the Na atom is adsorbed with a small height above the surface on an adsorption site like the cave as favored for K in the calculations of Ye, Freeman, and Delley,¹⁷ the Na-Si bond length would be rather horizontal. In this case, it is likely that the measurement of the Na-Si bond length would be easier using *s*-polarized PEXAFS since the electric vector of the incoming synchrotron radiation would be parallel to the Si(100)2×1 surface [Fig. 1(a)]. In that respect, our *s*-polarized PEXAFS results suggest that the Na is adsorbed on the Si(100)2×1 surface with a short height above the surface which would be again consistent with the cave adsorption site as proposed previously.¹⁷

In order to discriminate between the one-dimensional alkali-metal chain (ODAC) model as shown by STM for the K/Si(100)2×1 system¹³ and double-layer models,^{7–10,18–20} we have investigated the possibility of measuring the Na-Na distance between two chains, perpendicular to the $\langle 110 \rangle$ direction. In the case of the ODAC model (whatever is the adsorption site), the distance between Na chains would be 7.68 Å, which is too large a distance to be measured by any EXAFS technique since the EXAFS oscillations would be overshadowed by the noise. In the case of a two-layer model, the distance between two Na atoms located in two nearby layers would be close to 7.68/2, i.e., 3.84 Å (the distance between pedestal and cave is ≈ 4.4 Å and between pedestal and valley bridge is 3.9 Å), which is a distance that should be clearly resolved and give rise to EXAFS oscillations seen in *s*-polarized PEXAFS. Despite many measurements, we did not find any Na-Na bond length distance which could be consistent with any of the double-layer models. This suggests that, as shown for K/Si(100)2×1 by STM,^{11,13} Na is also likely to form one-dimensional chains parallel to the silicon dimer rows along the $\langle 110 \rangle$ direction, with a single site of adsorption.

One has now to use the distances obtained above to identify more directly the Na adsorption site. Let us first examine the case of a cave adsorption site. From Table I, one can see that the Na-Si bond length is 2.67 ± 0.05 Å [$R_1(\text{Na})$ from Na 2*p* PEXAFS and $R_2(\text{Si})$ from Si 2*p* PEXAFS in Table I], the Si-Si dimer bond length on the Na-covered surface is 2.44 ± 0.04 Å [$R_1(\text{Si})$ from Si 2*p* PEXAFS in Table I], and that the distance between a Na atom and the fourth Si nearest-neighbor distance is 5.10 ± 0.10 Å [$R_2(\text{Na})$ from Na 2*p* PEXAFS in Table I]. Since the PEXAFS data are collected in *s* polarization, the contribution of the two top atomic layers would be significantly dominant and the sensibility would be best for direction of bond lengths close to that of the electric vector (see Fig. 1). If we now calculate the distance from the Na atom to the fourth Si neighbor (d_4 in Fig. 9) using the Na-Si bond length (d_1 in Fig. 9) at 2.67 ± 0.05 Å and the Si-Si dimer bond length at 2.44 ± 0.04 Å, one obtains a value of 4.99 ± 0.09 Å, which corresponds exactly (within the errors) to the values obtained directly by PEXAFS (Table I) at $R_2(\text{Na}) = 5.10 \pm 0.10$ Å and by

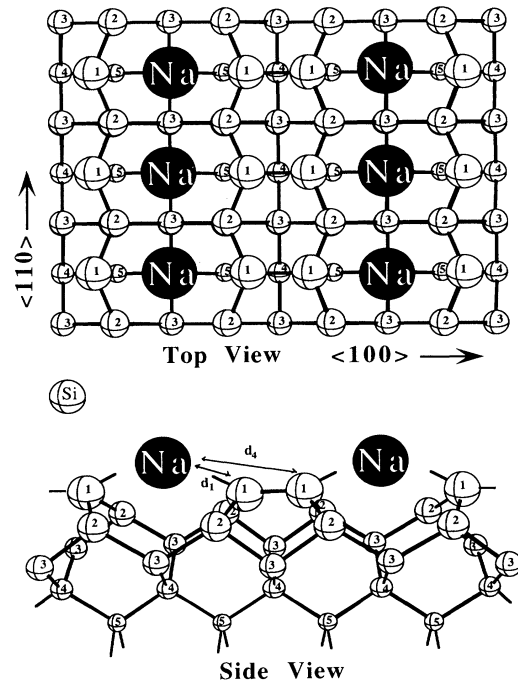


FIG. 9. Structural model proposed in this work for the adsorption of Na on the Si(100)2×1 surface (top and side views). The Na atoms are adsorbed on cave sites and form one-dimensional linear chains parallel to the Si dimer rows along the $\langle 110 \rangle$ direction and distant by 7.68 Å as shown in the top view. The numbers on the atoms indicate the atomic layers from the surface towards the bulk. On the side view, d_1 and d_4 indicate the distances between Na and, respectively, the first and fourth nearest Si atoms.

DMOL calculations at 5.11 Å. Let us now examine the cases of the valley-bridge and pedestal adsorption sites as done above for the cave site. The closest Na-Si distances from the value of 5.10 Å for the fourth nearest neighbor would be at 5.5 and 6.1 Å for the valley-bridge site, while for a pedestal adsorption site the closest corresponding distances would be 6.3 and 6.9 Å. These distances are clearly larger than the one obtained from the $R_2(\text{Na})$ Na 2*p* PEXAFS (Table I). We could therefore distinctly conclude that the cave is the Na adsorption site, which is further confirmed by its lowest adsorption energy (Table II). This finding is in very good agreement with the fact that the Na atoms are covalently bonded to Si atoms through the Si dangling bonds as shown by photoemission experiments,²⁶ which would also make the cave site the most favorable adsorption site—see Fig. 9. In that respect, our present PEXAFS and DMOL investigation for the Na/Si(100)2×1 agrees very well with the very recent STM study of the K/Si(100)2×1 system.¹³

VII. CONCLUSIONS

In conclusion, we have investigated the 1-ML Na/Si(100)2×1 system by the combination of *s*-polarized photoemission EXAFS experimental technique and

DMOL total-energy molecular calculations. We have used the unique ability of PEXAFS to measure both adsorbate and substrate nearest-neighbor distances, which allows a double checking of the bond lengths. We have measured the Si-Si dimer distance on the clean surface to be 2.20 ± 0.05 Å and its relaxation by 0.24 Å upon Na adsorption in excellent agreement with total-energy molecular DMOL calculations. The Si-Na (Si $2p$ PEXAFS) and Na-Si (Na $2p$ PEXAFS) distances were found to be strictly equal at 2.6 ± 0.05 Å, corresponding to the sum of covalent radii, which supports the model of covalent bonding between Na and Si proposed on the basis of photoemission experiments. Together with the other Na-Si and Si-Si bond lengths, also in very good agreement with the calculations, the measured distances clearly indicate that Na is adsorbed on a single site, the cave site. We did not find any Na-Na distances perpendicular to the $\langle 110 \rangle$ direction which could be consistent with any of the double-layer models. Calculations of adsorption energies further support the cave site. Our structural model for the Na/Si(100) 2×1 , based on the combination of these theoretical and experimental investigations, is in excellent agreement with the one we have recently proposed for the corresponding K/Si(100) 2×1 system on the basis of

a very different experimental technique, the scanning tunneling microscopy. Our investigation shows that the combination of new sophisticated experimental techniques with state-of-the-art theoretical approaches brings deeper insights into the understanding of the structure of surfaces and interfaces.

ACKNOWLEDGMENTS

This project was supported by the U.S. National Science Foundation under Contract No. DMR 92-23710 at Northern Illinois University, by the Ministère de la Recherche et de l'Espace at Commissariat à l'Energie Atomique, by the U.S. Office of Naval Research under Grant No. N0004-895-1290, and by a computing grant at the U.S. Naval Oceanographic Office, Stennis Space Center, Mississippi at Northwestern University. This work is based upon research conducted in part at the Synchrotron Radiation Center, University of Wisconsin-Madison which is supported by the U.S. National Science Foundation under Contract No. DMR92-12658. We thank the technical staff of the Synchrotron Radiation Center for expert and outstanding assistance.

*Also at Department of Physics, Northern Illinois University, DeKalb, Illinois 60115-2854.

†Permanent address: Commissariat à l'Energie Atomique, Service de Recherche sur les Surfaces et l'Irradiation de la Matière, Bâtiment 462, Centre d'Etudes de Saclay, 91191 Gif sur Yvette CEDEX, France and Département de Physique, Université de Paris-Sud, 91405 Orsay CEDEX, France.

¹*Physics and Chemistry of Alkali Metals Adsorption*, edited by H. P. Bonzel, A. M. Bradshaw, and G. Ertl, Materials Science Monographs Vol. 57 (Elsevier, Amsterdam, 1989), and references therein.

²*Metallization and Metal/Semiconductor Interfaces*, Vol. 195 of *NATO Advanced Study Institute, Series B: Physics*, edited by I. P. Batra (Plenum, New York, 1989), and references therein.

³P. Soukiassian, in *Fundamental Approach to New Materials Phases—Ordering at Surfaces and Interfaces*, edited by A. Yoshimori, T. Shinjo, and H. Watanabe, Springer Series in Materials Science Vol. 17 (Springer-Verlag, Berlin, 1992), p. 197, and references therein.

⁴J. Levine, *Surf. Sci.* **34**, 90 (1973).

⁵H. Tochiyama, *Surf. Sci.* **126**, 523 (1983).

⁶C. M. Wei, H. Huang, S. Y. Tong, G. S. Glander, and M. B. Webb, *Phys. Rev. B* **42**, 11 284 (1990).

⁷T. Abukawa and S. Kono, *Phys. Rev. B* **37**, 9097 (1988); *Surf. Sci.* **214**, 141 (1989).

⁸T. Makita, S. Kohmoto, and A. Ichimiya, *Surf. Sci.* **242**, 65 (1991).

⁹A. J. Smith, W. R. Graham, and E. W. Plummer, *Surf. Sci. Lett.* **243**, L37 (1991).

¹⁰E. G. Michel, P. Pervan, G. R. Castro, R. Miranda, and K. Wandelt, *Phys. Rev. B* **45**, 11 811 (1992).

¹¹P. Soukiassian and J. A. Kubby, in *Structure of Surfaces-III*, edited by S. Y. Tong, X. Xide, K. Tagayanaki, and M. A. Van Hove, Springer Series in Surface Science Vol. 24 (Springer-Verlag, Berlin, 1991), p. 584; J. A. Kubby, W. J. Greene, and

P. Soukiassian, *J. Vac. Sci. Technol. B* **9**, 739 (1991).

¹²U. A. Effner, D. Badt, J. Binder, T. Bertrams, A. Brodde, Ch. Lunau, H. Neddermeyer, and M. Hanbücken, *Surf. Sci.* **277**, 207 (1992).

¹³P. Soukiassian, J. A. Kubby, P. S. Mangat, Z. Hurych, and K. M. Schirm, *Phys. Rev. B* **46**, 13 471 (1992).

¹⁴T. Kendelewicz, P. Soukiassian, R. S. List, J. C. Woicik, P. Pianetta, I. Lindau, and W. E. Spicer, *Phys. Rev. B* **37**, 7115 (1988).

¹⁵S. T. Kim, P. Soukiassian, L. Barbier, S. Kapoor, and Z. Hurych, *Phys. Rev. B* **44**, 5622 (1991).

¹⁶V. Eteläniemi, E. G. Michel, and G. Materlik, *Phys. Rev. B* **44**, 4036 (1991); S. Lagomarsino, F. Scarinci, P. Castrucci, C. Giannini, E. Fontes, and J. R. Patel, *ibid.* **46**, 13 631 (1992).

¹⁷Ye Ling, A. J. Freeman, and B. Delley, *Phys. Rev. B* **39**, 10 144 (1989).

¹⁸I. P. Batra, *Phys. Rev. B* **39**, 3919 (1989).

¹⁹Y. Morikawa, K. Kobayashi, K. Terakura, and S. Blügel, *Phys. Rev. B* **44**, 3459 (1991).

²⁰B. L. Zhang, C. T. Chan, and K. M. Ho, *Phys. Rev. B* **44**, 8210 (1991).

²¹G. M. Rothberg, K. M. Choudhary, M. L. den Boer, G. P. Williams, M. H. Hecht, and I. Lindau, *Phys. Rev. Lett.* **53**, 1183 (1984).

²²K. M. Choudhary, P. S. Mangat, H. I. Starnberg, Z. Hurych, D. Kilday, and P. Soukiassian, *Phys. Rev. B* **39**, 759 (1989).

²³P. S. Mangat, K. M. Choudhary, D. Kilday, and G. Margaritondo, *Phys. Rev. B* **44**, 6284 (1991).

²⁴P. S. Mangat, Ph.D. thesis, University of Notre Dame, Indiana, 1991; P. S. Mangat, S. T. Kim, K. M. Choudhary, Z. Hurych, and P. Soukiassian, *Surf. Sci.* **285**, 102 (1993).

²⁵P. Soukiassian, T. M. Gentle, M. H. Bakshi, A. S. Bommanavar, and Z. Hurych, *Phys. Scr.* **35**, 757 (1987).

²⁶P. Soukiassian, M. H. Bakshi, Z. Hurych, and T. M. Gentle, *Surf. Sci. Lett.* **221**, L759 (1989).

- ²⁷P. Soukiassian and T. Kendelewicz, in *Metallization and Metal/Semiconductor Interfaces*, Ref. 2, p. 465.
- ²⁸P. Soukiassian, K. M. Schirm, P. S. Mangat, and Z. Hurych, *Bull. Am. Phys. Soc.* **37**, 224 (1992).
- ²⁹L. Spiess, P. S. Mangat, S. P. Tang, K. M. Schirm, A. J. Freeman, and P. Soukiassian, *Surf. Sci. Lett.* **289**, L631 (1993).
- ³⁰B. Delley, *J. Chem. Phys.* **92**, 508 (1990); **94**, 7245 (1991).
- ³¹Density Functional Molecular Program—DMOL Biosym Technologies Inc., San Diego, California.
- ³²S. P. Tang, A. J. Freeman, and B. Delley, *Phys. Rev. B* **45**, 1776 (1992), and references therein.
- ³³K. Kobayashi, Y. Morikawa, K. Terakura, and S. Blügel, *Phys. Rev. B* **45**, 3469 (1992).
- ³⁴J. Stöhr, R. S. Bauer, J. C. McMennamin, L. I. Johansson, and S. Brennan, *J. Vac. Sci. Technol.* **16**, 1195 (1980); also J. Stöhr (unpublished).
- ³⁵B. K. Teo and P. A. Lee, *J. Am. Chem. Soc.* **101**, 2815 (1979); *EXAFS Spectroscopy: Techniques and Applications*, edited by B. K. Teo and D. C. Joy (Plenum, New York, 1982).
- ³⁶A. G. McKale, B. W. Veal, A. P. Paulikas, S. K. Chan, and G. S. Knapp, *J. Am. Chem. Soc.* **110**, 3763 (1988).
- ³⁷I. P. Batra, *Phys. Rev. B* **41**, 5048 (1990).
- ³⁸One should notice that the d_1 bond length determined by DMol calculations depends strongly on the Na height above the surface. Since the Na-Si bonding is weak, the Na height is determined with less accuracy as for a strong bonding like the dimer bond. This might explain somehow why the calculated bond length d_1 appears slightly overestimated as compared to the PEXAFS distance for the corresponding bond length; see Ref. 29.
- ³⁹We should mention that we have also investigated the effect of the number of Na atoms on the value of the dimer bond length after relaxation in the case of the cave adsorption site. While our calculation indicates a relaxation of 0.04 Å with a single Na atom, we obtain a value of 0.14 Å when using two Na atoms as shown in this paper. This last value is in good agreement with the experimental PEXAFS value at 0.24 Å.